JOURNAL OF SOLID STATE CHEMISTRY **110**, 1–5 (1994)

$Rb_4Al_2Nb_{35}O_{70}$: A New Reduced Niobate with Isolated Nb_6 Octahedral Clusters

Margret J. Geselbracht and Angelica M. Stacy*

Department of Chemistry, University of California Berkeley, Berkeley, California 94720

Received December 22, 1992; in revised form April 20, 1993; accepted April 23, 1993

Single crystals of the new reduced niobium oxide, $Rb_4Al_2Nb_{35}O_{70}$, were grown by heating mixtures of Na_3NbO_4, NbO, and RbCl in an alumina boat, sealed in a fused silica tube. $Rb_4Al_2Nb_{35}O_{70}$ crystallizes in the trigonal space group $P\bar{3}$: $a = 7.815(1)$ Å, $c = 26.392(9)$ Å, with one formula unit per unit cell. The structure was determined from single crystal X-ray diffraction data and refined to an R value of 3.39%. Three distinct types of niobium atom coordination environments exist in this structure including isolated NbO_6 octahedra, Nb_3O_{13} triangular clusters formed by 3 face-shared NbO_6 octahedra, and Nb_6 octahedral clusters of the type $[Nb_6O_{12}]O_6$. © 1994 Academic Press, Inc.

INTRODUCTION

The presence of metal–metal bonding in many reduced early transition metal oxides leads to a very diverse structural chemistry. Both niobium and molybdenum frequently form M_6O_{12}-octahedral clusters with very short intermetallic distances within a cluster (1). In the reduced oxomolybdates, the Mo_6O_{12}-octahedral clusters are usually condensed by edge-sharing into oligomeric chains. In contrast to the oxomolybdates, there are many examples now known of reduced oxoniobates in which the Nb_6O_{12}-octahedral clusters are found as discrete units (2–8). A few examples of new materials containing corner-sharing Nb_6O_{12}-octahedral clusters also have been reported recently (9–11). Here we report the preparation of single crystals of a new reduced niobium oxide, $Rb_4Al_2Nb_{35}O_{70}$, which belongs to the class of materials with discrete Nb_6O_{12}-octahedral clusters. Three distinct types of niobium atom coordination environments exist in this structure including isolated NbO_6 octahedra, Nb_3O_{13} triangular clusters formed by 3 face-shared NbO_6 octahedra, and Nb_6 octahedral clusters of the type $[Nb_6O_{12}]O_6$.

Single crystals of reduced niobates have been relatively difficult to obtain. Many of the new phases that have been reported are polycrystalline samples that have been studied by using electron microscopy and powder diffraction methods (9, 11, 12). One successful method of obtaining crystals is to add a small amount of NaF or B_2O_3 to the reaction mixture as a mineralizing agent. This has led to a number of new materials including $Na_3Al_2Nb_{34}O_{64}$ (4), $Na(Si,Nb)Nb_{10}O_{19}$ (4), and $NaNb_{10}O_{18}$ (13). Recently, the use of fluxes has been described to obtain single crystals of new reduced barium niobates. A barium borate flux led to the preparation of large single crystals of $Ba_2Nb_{15}O_{32}$ (14), while a $BaCl_2$ flux was used to prepare the complex oxide, $BaNb_{10}SiO_{19}$ (15). We report here the use of molten rubidium chloride as a flux to grow crystals of $Rb_4Al_2Nb_{35}O_{70}$. The structure of this material was determined by using single crystal X-ray diffraction methods as described below.

EXPERIMENTAL

Na_3NbO_4 was prepared from Na_2CO_3 (Fisher) and Nb_2O_5 (Cerac, 99.95%) at 950°C. NbO was synthesized from the reaction of Nb (Cerac, 99.8%) and Nb_2O_5 in an evacuated sealed fused silica tube at 1100°C. Single crystals of $Rb_4Al_2Nb_{35}O_{70}$ were obtained as follows: a 1 : 1 molar ratio of Na_3NbO_4 and NbO was mixed with a 10-fold excess, by weight, of RbCl (Aldrich, 99+%), placed in an alumina combustion boat, and sealed in an evacuated fused silica tube. The tube was heated from room temperature to 1050°C over 4 hr, held at 1050°C for 12 hr, cooled to 700°C (mp RbCl = 718°C) over 36 hr and finally cooled to room temperature over 10 hr. The RbCl flux was removed by repeated washings with triply deionized water, leaving a mixture of polycrystalline powder and metallic gold crystals. These crystals grew in the shapes of hexagonal and triangular plates and were easily separated for further characterization. Energy dispersive spectroscopy (EDS) performed in a scanning electron microscope was used to qualitatively determine the cations present; rubidium, aluminum, and niobium were detected, but sodium was absent.

Single-crystal intensity data were collected on an Enraf-

---

* To whom correspondence should be addressed.

0022-4596/94 $6.00

Nonius CAD-4 diffractometer at 25°C (16). Mo$K\alpha$ radiation (λ = 0.71073 Å) and a monochromator of highly oriented graphite (2θ = 12.2°) were used. Automatic peak search and indexing procedures yielded a primitive trigonal cell, which was used for all further work. Unit cell parameters, a = 7.815(1) Å and c = 26.392 (9) Å were refined on the setting angles of 24 reflections with 2θ greater than 22°. Other relevant crystal parameters are summarized in Table 1.

Intensities for 3427 reflections were measured ($\pm h$, $+k$, $+l$, $3° < 2\theta < 55°$) at 25°C for a crystal of $Rb_4Al_2Nb_{35}O_{70}$ and converted to structure factor amplitudes and their esd's by correction for scan speed, background, and Lorentz and polarization effects (17, 18). Correction for absorption was based on the azimuthal data, (19) which showed a variation I_{min}/I_{max} = 0.56 for the average curve. No systematic absences were observed. Possible space groups were $P3$ or $P\bar{3}$. Refinement of the structure was successful in $P\bar{3}$, so $P3$ was not considered. Averaging yielded 2056 unique reflections. The R value of agreement (20) based on intensity was 6.8% and on structure factors was 3.4%.

The metal atom positions were solved by direct methods, (21) and the oxygen atom positions determined by difference Fourier techniques (see Table 2). This structural model was then refined via standard least-squares and Fourier techniques. All atoms except the oxygen atoms were refined with anisotropic thermal parameters. The final residuals for 112 variables refined against the 1667 independent reflections for which $F^2 > 3\sigma(F^2)$ were R = 3.39%, R_W = 4.67%, and GOF = 1.635. The R value for all 2056 retained data was 5.22%. The quantity minimized by the least-squares routine was $\Sigma w(|F_o| - |F_c|)^2$, where w is the weight of a given observation. The secondary extinction parameter g was refined also (22), and its value is given in Table 1. The maximum correction, gI_{max}, was 0.20. The final refinement cycle converged with a shift/error <0.03, and the largest peak in the difference Fourier had an absolute value of electron density of 2.12 electrons/Å^3. The p factor used to reduce the weight of the intense reflections was set to 0.03 in the final stages of refinement. The analytical forms of the scattering factors for the neutral atoms were used (23), and all scattering factors were corrected for both the real and imaginary components of the anomalous dispersion (24). A list of the values of F_o and F_c is available as supplementary material.

TABLE 1

Crystal Parameters at 25°C for $Rb_4Al_2Nb_{35}O_{70}$

a = 7.815(1) Å
b = 7.815(1) Å
c = 26.392(9) Å
$\alpha = \beta = 90°$
γ = 120°
V = 1395.6(7) Å^3
Z = 1
f_W = 4767.5
Space group: $P\bar{3}$ (No. 147)

crystal size: 0.15 × 0.12 × 0.06 mm
λ = 0.71073 Å
ρ_{calc} = 5.67 g cm^{-3}
μ_{calc} = 101 cm^{-1}
I_{min}/I_{max} = 0.56
g = 2.05(6) 10^{-7}
$R(F^2)$ = 3.39%
$R_W(F^2)$ = 4.67%
GOF = 1.635

TABLE 2

Positional Parameters and Their Estimated Standard Deviations

Atom	x	y	z	B_{iso} Å^{2a}
Nb1	0.60357(9)	0.87076(9)	0.09146(3)	0.33(1)
Nb2	0.45053(9)	0.13971(9)	0.18301(3)	0.25(1)
Nb3	0.64205(9)	0.11204(9)	0.27073(3)	0.26(1)
Nb4	0.5300(1)	0.6086(1)	0.36730(3)	0.69(2)
Nb5	0.80465(9)	0.02283(9)	0.45615(3)	0.28(1)
Nb6	0.000	0.000	0.000	0.62(2)
Nb7	0.000	0.000	0.18623(5)	0.30(2)
Nb8	0.333	0.667	0.53965(5)	0.68(2)
Rb1	0.000	0.000	0.32158(6)	1.28(2)
Rb2	0.333	0.667	0.96339(6)	0.81(2)
Al1	0.333	0.667	0.2065(2)	0.27(5)
O1	0.4314(7)	0.1275(7)	0.3179(2)	0.5(1)*
O2	0.0927(7)	0.5087(8)	0.2270(2)	0.38(9)*
O3	0.2163(8)	0.2052(8)	0.0443(2)	0.8(1)*
O4	0.5999(8)	0.0939(7)	0.4152(2)	0.60(9)*
O5	0.2353(7)	0.1587(7)	0.2284(2)	0.30(9)*
O6	0.4278(7)	0.1685(8)	0.4999(2)	0.48(9)*
O7	0.0639(7)	0.2368(7)	0.1434(2)	0.40(9)*
O8	0.0284(7)	0.2311(7)	0.4093(2)	0.6(1)*
O9	0.2926(8)	0.4301(7)	0.3279(3)	0.7(1)*
O10	0.5050(8)	0.6121(8)	0.0606(2)	0.65(9)*
O11	0.6363(7)	0.0990(7)	0.1365(2)	0.44(9)*
O12	0.333	0.667	0.1393(4)	0.2(1)*
O13	0.333	0.667	0.4045(4)	0.9(2)*

[a] Starred values indicate atoms were refined with isotropic thermal parameters.

RESULTS AND DISCUSSION

The use of molten RbCl as a flux has lead to crystals of the new reduced niobate, $Rb_4Al_2Nb_{35}O_{70}$. This material readily incorporates Rb from the flux and also dissolves Al from the Al_2O_3 reaction vessel. It is notable that the use of Na_3NbO_4 appears to be crucial in this synthesis, although Na is not present in the crystals. Attempts to make $Rb_4Al_2Nb_{35}O_{70}$ from stoichiometric amounts of NbO, NbO_2, and Al_2O_3 in a RbCl flux under the same heating conditions lead to no appreciable reaction of the binary compounds.

The structure of $Rb_4Al_2Nb_{35}O_{70}$ can be described as layers of metal atoms arranged in sheets perpendicular to the c axis. There are four layers of Rb atoms and two layers of Al atoms per unit cell. The remaining layers are comprised of Nb atoms.

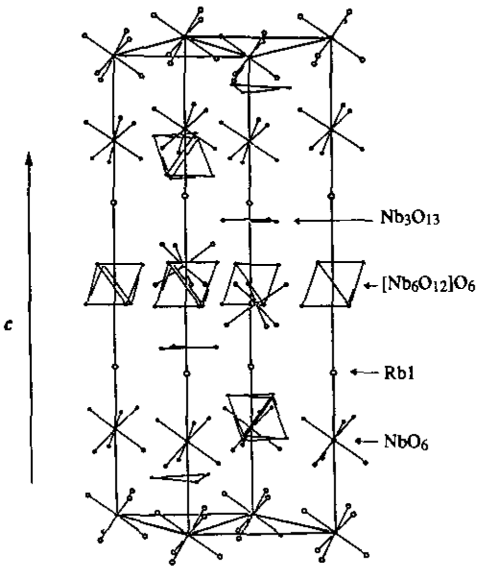

FIG. 1. View of the unit cell of $Rb_4Al_2Nb_{35}O_{70}$ showing the packing of the $[Nb_6O_{12}]O_6$ octahedral clusters, the Nb_3O_{13} triangular clusters, the NbO_6 octahedra, and the Rb1 atoms; one of each type of cluster is labeled on the diagram. The Al atoms and Rb2 atoms have been omitted, and only the O atoms in the NbO_6 octahedra are shown for clarity. To emphasize the distinct types of Nb coordination environments, Nb–O bonds in the NbO_6 octahedra and Nb–Nb bonds in the $[Nb_6O_{12}]O_6$ octahedral clusters are shown; in addition, nonbonding Nb–Nb contacts are drawn in the Nb_3O_{13} triangular clusters.

The Nb atoms are found in three distinct coordination environments: isolated NbO_6 octahedra; Nb_3O_{13} triangular clusters formed by 3 face-sharing NbO_6 octahedra; and Nb_6 octahedral clusters of the type $[Nb_6O_{12}]O_6$. The packing of these structural units is shown in Fig. 1. Metal-oxygen bond distances for Nb, Al, and Rb and short Nb–Nb bond distances are listed in Table 3; angles between the Nb and O atoms are listed in Table 4. Although the average oxidation state of Nb in this material is +3.7, the different coordination environments suggest two distinct formal oxidation states.

The isolated NbO_6 octahedra are located on the unit cell edges at $z \sim 0$ (Nb6) and at $z \sim 0.19$ and 0.81 (Nb7), and on the 3-fold axes at $z \sim 0.54$ (Nb8). The Nb–O bond distances in these octahedra are relatively short, ranging from 1.957(5) to 2.054(6) Å. These short bond distances indicate a formal oxidation state of +5 for the Nb atoms in these octahedra.

The triangular Nb_3O_{13} clusters containing Nb1 are located on the 3-fold axes at $z \sim 0.09$ and 0.91, and the triangular Nb_3O_{13} clusters containing Nb4 are located on the 3-fold axes at $z \sim 0.37$ and 0.63. Each Nb atom in these clusters is in a distorted octahedral environment; the three NbO_6 units share faces. In these triangular clusters, the Nb–O bond distance to the triply bridging O atom is elongated. This is most pronounced in the clusters containing Nb1, where the triply bridging O12 atom is also coordinated to an Al atom as shown in Fig. 2 (Nb1–O12 = 2.287(6) Å); the Nb–O bond trans to this elongated bond is significantly shorter (Nb1–O3 = 1.829(6) Å). Since the other four Nb–O distances are relatively short (ranging from 1.945(6) to 1.995(5) Å), we conclude that the formal oxidation state for the Nb atoms in these triangular clusters is +5. Additionally, the relatively long Nb–Nb distances of 3.130(1) and 3.303(1) Å within these clusters preclude any metal–metal bonding interactions.

The Nb_6 octahedral clusters located on the 3-fold axes at $z \sim 0.23$ and 0.77 (formed by Nb2 and Nb3) and on the unit cell edges at $z \sim 0.5$ (formed by Nb5) contain the reduced Nb atoms that are bonded to each other. This $[Nb_6O_{12}]O_6$ structural unit, shown in Fig. 3, is a very common structural feature of reduced niobium oxides. The existence of very short Nb–Nb contacts within the

TABLE 3
Selected Bond Distances and Their Estimated Standard Deviations (Å)

Nb1–O3	1.829(6)	Nb4–O4	1.967(5)	Rb1–O5 (×3)	2.947(6)
Nb1–O7	1.995(5)	Nb4–O8	2.033(6)	Rb1–O8 (×3)	2.876(6)
Nb1–O10	1.945(6)	Nb4–O9	1.970(5)	Rb1–O9 (×3)	2.978(5)
Nb1–O10	1.956(5)	Nb4–O9	2.120(7)	Rb2–O3 (×3)	3.147(6)
Nb1–O11	2.050(6)	Nb4–O13	2.056(5)	Rb2–O10	3.023(7)
Nb1–O12	2.287(6)	Nb5–O4	2.220(7)	Rb2–O10	3.081(7)
Nb2–O2	2.056(5)	Nb5–O6	2.040(5)	Rb2–O11	3.150(6)
Nb2–O5	2.129(6)	Nb5–O6	2.099(6)		
Nb2–O7	2.208(7)	Nb5–O8	2.095(5)	Al1–O2 (×3)	1.741(5)
Nb2–O11	2.044(6)	Nb5–O8	2.054(7)	Al1–O12	1772(11)
Nb2–O11	2.101(5)	Nb6–O3 (×6)	2.022(5)	Nb2–Nb2 (×2)	2.786(1)
Nb3–O1	2.114(6)	Nb7–O5 (×3)	1.969(5)	Nb2–Nb3	2.823(1)
Nb3–O1	2.083(6)	Nb7–O7 (×3)	2.006(6)	Nb2–Nb3	2.834(1)
Nb3–O2	2.046(6)	Nb8–O4 (×3)	2.054(6)	Nb3–Nb3 (×2)	2.843(1)
Nb3–O5	2.045(5)	Nb8–O6 (×3)	1.957(5)	Nb5–Nb5 (×2)	2.811(1)
Nb3–O9	2.302(7)	Rb1–P1 (×3)	3.002(6)	Nb5–Nb5 (×2)	2.827(1)
Nb4–O1	1.972(6)				

TABLE 4
Selected Bond Angles and Their Estimated Standard Deviations (°)

O3–Nb1–O7	100.2(2)	O1–Nb3–O1	91.4(2)	O4–Nb5–O6	88.3(2)
O3–Nb1–O10	96.8(3)	O1–Nb3–O2	89.1(2)	O4–Nb5–O6	79.4(2)
O3–Nb1–O10	98.4(2)	O1–Nb3–O2	175.9(2)	O4–Nb5–O8	86.8(2)
O3–Nb1–O11	99.4(3)	O1–Nb3–O5	88.9(2)	O4–Nb5–O8	96.6(2)
O3–Nb1–O12	170.6(3)	O1–Nb3–O5	175.3(2)	O6–Nb5–O6	89.6(2)
O7–Nb1–O10	93.8(3)	O1–Nb3–O9	78.2(2)	O6–Nb5–O8	91.4(2)
O7–Nb1–O10	160.3(2)	O1–Nb3–O9	88.6(2)	O6–Nb5–O8	87.9(2)
O7–Nb1–O11	86.2(3)	O2–Nb3–O5	90.2(2)	O6–Nb5–O8	174.9(3)
O7–Nb1–O12	86.5(2)	O2–Nb3–O9	87.6(2)	O6–Nb5–O8	175.9(2)
O10–Nb1–O10	90.4(3)	O5–Nb3–O9	97.1(2)	O8–Nb5–O8	90.8(2)
O10–Nb1–O11	163.5(2)				
O10–Nb1–O11	84.4(3)	O1–Nb4–O4	97.3(2)	O3–Nb6–O3	180.0(0)
O10–Nb1–O12	76.0(2)	O1–Nb4–O8	92.2(2)	O3–Nb6–O3	89.9(3)
O10–Nb1–O12	75.8(2)	O1–Nb4–O9	90.0(3)	O3–Nb6–O3	90.1(3)
O11–Nb1–O12	87.5(2)	O1–Nb4–O9	91.4(2)	O5–Nb7–O5	91.2(3)
O2–Nb2–O5	89.1(2)	O1–Nb4–13	167.0(3)	O5–Nb7–O7	86.7(3)
O2–Nb2–O7	89.0(2)	O4–Nb4–O8	87.1(3)	O5–Nb7–O7	90.8(2)
O2–Nb2–O11	89.5(2)	O4–Nb4–O9	93.3(3)	O5–Nb7–O7	177.1(3)
O2–Nb2–O11	175.6(3)	O4–Nb4–O9	169.4(2)	O7–Nb7–O7	91.4(2)
O5–Nb2–O7	77.9(2)	O4–Nb4–O13	93.6(3)		
O5–Nb2–O11	174.8(2)	O8–Nb4–O9	86.4(2)	O4–Nb8–O4	89.7(2)
O5–Nb2–O11	88.8(2)	O8–Nb4–O9	177.7(3)	O4–Nb8–O6	89.2(2)
O7–Nb2–O11	97.0(2)	O8–Nb4–O13	95.5(2)	O4–Nb8–O6	86.9(3)
O7–Nb2–O11	86.7(2)	O9–Nb4–O9	92.8(2)	O4–Nb8–O6	176.4(2)
O11–Nb2–O11	92.2(2)	O9–Nb4–O13	82.2(3)	O6–Nb8–O6	94.2(3)
		O9–Nb4–O13	78.7(2)		

octahedral cluster, ranging from 2.786(1) to 2.843(1) Å, indicates metal–metal bonding. For comparison, the Nb–Nb distance in niobium metal is 2.85 Å (25).

The intracluster Nb–Nb distances between the Nb_6 octahedral clusters are much longer. In contrast to many related materials, the clusters do not share any oxygen atoms and are truly isolated from one another. For example, the layer of Nb_6 octahedral clusters formed by Nb5 is in a pseudohexagonal close packed arrangement with NbO_6 octahedra. This isolation of clusters is presumably due to the fact that the average oxidation state of Nb in this structure of +3.7 is much higher than the value of

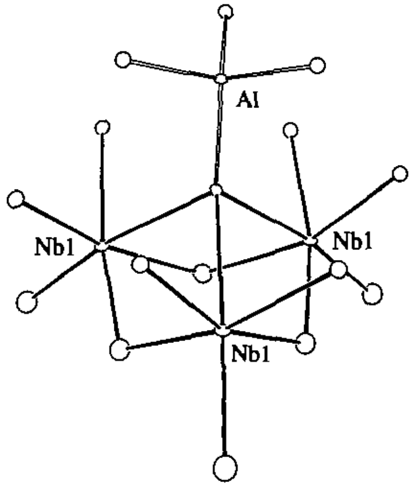

FIG. 2. Perspective ORTEP diagram of the Nb_3O_{13} triangular cluster formed by Nb1 and the associated Al atom, showing 50% probability ellipsoids. Nb–O bonds are shaded; Al–O bonds are unshaded.

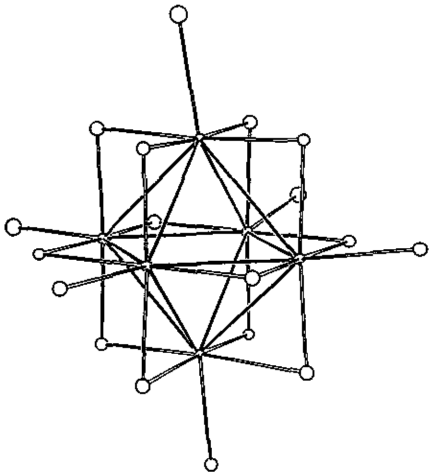

FIG. 3. Perspective ORTEP diagram showing the $[Nb_6O_{12}]O_6$ octahedral cluster. Nb–Nb bonds are shaded; Nb–O bonds are unshaded. Thermal ellipsoids are drawn at the 50% probability level.

+2.75 which has been observed in most of the structures with $[Nb_6O_{12}]O_6$ octahedral clusters reported previously. Assuming the coordination environment to be indicative of the formal oxidation state, $Rb_4Al_2Nb_{35}O_{70}$ can be written in the ionic limit as $Rb_4^{1+}Al_2^{3+}Nb_5^{5+}(Nb_3^{5+})_4(Nb_6^{2.5+})_3O_{70}^{2-}$; each $[Nb_6O_{12}]O_6$ cluster then has 15 valence e^-'s. Clusters of this type generally have 14–16 valence e^-'s to participate in metal–metal bonding (1).

The other cations in this structure have coordination environments that are not surprising. The Al atoms are located on the 3-fold axes at $z \sim 0.21$ and 0.79 in the center of a distorted C_{3v} tetrahedron of oxygen atoms (Fig. 2). Three Al–O distances are 1.741(5) Å and one distance is 1.772(11) Å. Both types of Rb atoms are 12-coordinate. Rb1 forms discrete layers with the atoms located on the unit cell edges at $z \sim 0.32$ and 0.68, and Rb2 is located on the three-fold axes at $z \sim 0.04$ and 0.96. For both types of Rb atoms, the Rb–O bond lengths range from 2.947(6) Å to 3.150(6) Å.

Two complex reduced niobium oxides which are related structurally to $Rb_4Al_2Nb_{35}O_{70}$ are $Ba_2Nb_{15}O_{32}$ (14) and $BaNb_{10}SiO_{19}$ (15). All three of these materials have complex structures in which the Nb atoms are located in three different coordination environments: isolated NbO_6 octahedra, Nb_3O_{13} triangular clusters, and $[Nb_6O_{12}]O_6$ octahedral clusters. The average oxidation states of the Nb atoms in these materials range from +3.2 for $BaNb_{10}SiO_{19}$, to +3.7 for $Rb_4Al_2Nb_{35}O_{70}$, and +4 for $Ba_2Nb_{15}O_{32}$. In $BaNb_{10}SiO_{19}$, the reduced Nb atoms are found not only in the $[Nb_6O_{12}]O_6$ octahedral clusters, but also in the Nb_3O_{13} triangular clusters as indicated by the short Nb–Nb bonds ($d_{\text{Nb-Nb}} = 2.829(3)$ Å). The electrical properties of $BaNb_{10}SiO_{19}$ and $Ba_2Nb_{15}O_{32}$ have been studied, and both of these materials are reported to be semiconductors.

A material which is more closely related to $Rb_4Al_2Nb_{35}O_{70}$ in composition is $Na_3Al_2Nb_{34}O_{64}$ (4) with an average Nb oxidation state of +3.5. The sodium material also contains isolated NbO_6 octahedra and $[Nb_6O_{12}]O_6$ octahedral clusters, but in addition has Nb_2O_{10} dumbell units with very short Nb–Nb contacts ($d_{\text{Nb-Nb}} = 2.685$ Å). No further characterization of $Na_3Al_2Nb_{34}O_{64}$ has been reported.

In summary, $Rb_4Al_2Nb_{35}O_{70}$ is a new member of a rich family of reduced niobates in which the Nb atoms are in more than one coordination environment. In $Rb_4Al_2Nb_{35}O_{70}$, the reduced Nb atoms are found in $[Nb_6O_{12}]O_6$ octahedral clusters, and the Nb^{5+} atoms in NbO_6 octahedra and in Nb_3O_{13} triangular clusters. Compared with more reduced members of the family, the $[Nb_6O_{12}]O_6$ octahedral clusters are isolated in $Rb_4Al_2Nb_{35}O_{70}$, and there are no Nb–Nb bonds in the Nb_3O_{13} triangular clusters.

ACKNOWLEDGMENT

This work was supported by the National Science Foundation (Grant DMR-9102492).

REFERENCES

1. (a) J. Köhler, G. Svensson, and A. Simon *Angew. Chem. Int. Ed.* **31,** 1437 (1992). (b) A. Simon, *Angew. Chem. Int. Ed.* **27,** 159 (1988).
2. D. M. Evans and L. Katz, *J. Solid State Chem.* **6,** 459 (1973).
3. (a) B. O. Marinder, *Chem. Scr.* **11,** 97 (1977); (b) R. Burnus, J. Köhler, and A. Simon, *Z. Naturforsch. B* **42,** 536 (1987).
4. J. Köhler, and A. Simon, *Z. Anorg. Allg. Chem.* **553,** 106 (1987).
5. J. Köhler, G. Miller, and A. Simon, *Z. Anorg. Allg. Chem.* **568,** 8 (1989).
6. J. Köhler, A. Simon, S. J. Hibble, and A. K. Cheetham, *J. Less-Common Met.* **142,** 123 (1988).
7. S. J. Hibble, A. K. Cheetham, J. Köhler, and A. Simon, *J. Less-Common Met.* **154,** 271 (1989).
8. J. Köhler, and A. Simon, *Z. Anorg. Allg. Chem.* **572,** 7 (1989).
9. G. Svensson, *Mat. Res. Bull.* **23,** 437 (1988).
10. A. Simon, J. Köhler, R. Tischtau, and G. Miller, *Angew. Chem. Int. Ed.* **28,** 1662 (1989).
11. G. Svensson, *J. Solid State Chem.* **90,** 249 (1991).
12. S. J. Hibble, A. K. Cheetham, and D. E. Cox, *Inorg. Chem.* **26,** 2389 (1987).
13. J. Köhler, and A. Simon, *Z. Anorg. Allg. Chem.* **572,** 7 (1989).
14. S. A. Sunshine, B. Hessen, T. Siegrist, A. T. Fiory, and J. V. Waszczak, "NIST SP-804, Chemistry of Electronic Ceramic Materials," Proceedings of the international conference held in Jackson, WY, August 17–22, 1990, issued January 1991.
15. K. B. Kersting and W. Jeitschko, *J. Solid State Chem.* **93,** 350 (1991).
16. University of California Berkeley Chemistry Department X-ray Crystallographic Facility (CHEXRAY). Enraf-Nonius software is described in: "CAD4 Operation Manual." Enraf-Nonius: Delft, The Netherlands, November, 1977; updated January, 1980, et seq.
17. Calculations were performed on DEC MicroVax computers using locally modified versions of the Enraf-Nonius MolEN structure solution and refinement package and other programs.
18. MolEN—1990, Delft Instruments, X-ray Diffraction D.V., Rontgenweg 1, 2624 BD Delft, The Netherlands.
19. Reflections used for the azimuthal scans were located near $\chi = 90°$, and the intensities were sured at 10° increments of rotation of the crystal about the diffraction vector.
20. $R(I) = (\Sigma|I_{av}| - |I_i|)/\Sigma|I_i|$, where I_i are the individual measurements and I_{av} the average to which the individual measurements contribute.
21. G. Sheldrick, SHELXS-86.
22. W. H. Zachriasen, *Acta Crystallogr.* **16,** 1139 (1963).
23. D. T. Cromer and J. T. Waber, *in* "International Tables for X-ray Crystallography" (J. A. Ibers and W. C. Hamilton, Eds.), Vol. IV, Table 2.2B. Kynoch, Birmingham (1974).
24. D. T. Cromer, in "International Tables for X-ray Crystallography" (J. A. Ibers and W. C. Hamilton, Eds.), Vol. IV, Table 2.3.1. Kynoch, Birmingham (1974).
25. N. N. Greenwood and A. Earnshaw, "Chemistry of the Elements," p. 1145, Pergamon, New York (1984).